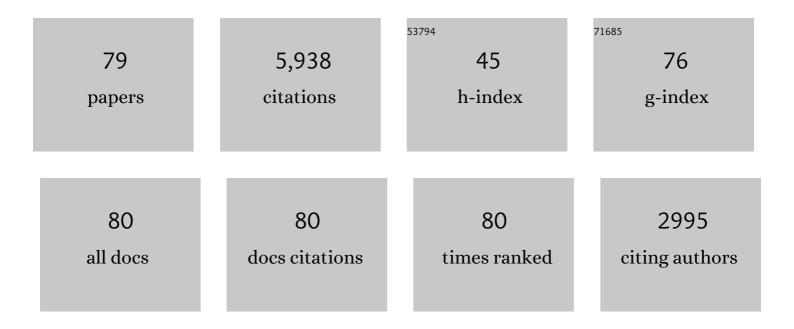
Dave J Waters

List of Publications by Year in descending order

Source: https://exaly.com/author-pdf/1967228/publications.pdf Version: 2024-02-01



#	Article	IF	CITATIONS
1	The structural geometry, metamorphic and magmatic evolution of the Everest massif, High Himalaya of Nepal–South Tibet. Journal of the Geological Society, 2003, 160, 345-366.	2.1	306
2	Tectonic evolution of the Mogok metamorphic belt, Burma (Myanmar) constrained by U-Th-Pb dating of metamorphic and magmatic rocks. Tectonics, 2007, 26, n/a-n/a.	2.8	278
3	Quantifying geological uncertainty in metamorphic phase equilibria modelling; a Monte Carlo assessment and implications for tectonic interpretations. Geoscience Frontiers, 2016, 7, 591-607.	8.4	256
4	Plate velocity exhumation of ultrahigh-pressure eclogites in the Pakistan Himalaya. Geology, 2006, 34, 989.	4.4	195
5	Dating the geologic history of Oman's Semail ophiolite: insights from U-Pb geochronology. Contributions To Mineralogy and Petrology, 2005, 150, 403-422.	3.1	184
6	Structural evolution, metamorphism and restoration of the Arabian continental margin, Saih Hatat region, Oman Mountains. Journal of Structural Geology, 2004, 26, 451-473.	2.3	172
7	Two episodes of monazite crystallization during metamorphism and crustal melting in the Everest region of the Nepalese Himalaya. Geology, 2000, 28, 403.	4.4	158
8	Timing of Midcrustal Metamorphism, Melting, and Deformation in the Mount Everest Region of Southern Tibet Revealed by U(â€Th)â€Pb Geochronology. Journal of Geology, 2009, 117, 643-664.	1.4	158
9	Metamorphism, Melting, and Extension: Age Constraints from the High Himalayan Slab of Southeast Zanskar and Northwest Lahaul. Journal of Geology, 1999, 107, 473-495.	1.4	152
10	The History of Granulite-Facies Metamorphism and Crustal Growth from Single Zircon U-Pb Geochronology: Namaqualand, South Africa. Journal of Petrology, 1999, 40, 1747-1770.	2.8	150
11	The significance of prograde and retrograde quartz-bearing intergrowth microstructures in partially melted granulite-facies rocks. Lithos, 2001, 56, 97-110.	1.4	148
12	Assessing the extent of disequilibrium and overstepping of prograde metamorphic reactions in metapelites from the Bushveld Complex aureole, South Africa. Journal of Metamorphic Geology, 2002, 20, 135-149.	3.4	147
13	Hercynite-quartz granulites: phase relations, and implications for crustal processes. European Journal of Mineralogy, 1991, 3, 367-386.	1.3	140
14	Geochronology of granulitized eclogite from the Ama Drime Massif: Implications for the tectonic evolution of the South Tibetan Himalaya. Tectonics, 2009, 28, .	2.8	133
15	Integrated pressure–temperature–time constraints for the <scp>T</scp> so <scp>M</scp> orari dome (<scp>N</scp> orthwest <scp>I</scp> ndia): implications for the burial and exhumation path of <scp>UHP</scp> units in the western <scp>H</scp> imalaya. Journal of Metamorphic Geology, 2013, 31, 469-504.	3.4	133
16	Eclogitization of the Monviso ophiolite (W. Alps) and implications on subduction dynamics. Journal of Metamorphic Geology, 2012, 30, 37-61.	3.4	126
17	Structure and metamorphism of blueschist–eclogite facies rocks from the northeastern Oman Mountains. Journal of the Geological Society, 1994, 151, 555-576.	2.1	115
18	Crustal melt granites and migmatites along the Himalaya: melt source, segregation, transport and granite emplacement mechanisms. Earth and Environmental Science Transactions of the Royal Society of Edinburgh, 2009, 100, 219-233.	0.3	114

#	Article	IF	CITATIONS
19	Pressure, temperature and time constraints on Himalayan metamorphism from eastern Kashmir and western Zanskar. Journal of the Geological Society, 1992, 149, 753-773.	2.1	109
20	Telescoping of isotherms beneath the South Tibetan Detachment System, Mount Everest Massif. Journal of Structural Geology, 2011, 33, 1569-1594.	2.3	106
21	Inverted metamorphism and the Main Central Thrust: field relations and thermobarometric constraints from the Kishtwar Window, NW Indian Himalaya. Journal of Metamorphic Geology, 2000, 18, 571-590.	3.4	103
22	<i>P–T–t–D</i> paths of Everest Series schist, Nepal. Journal of Metamorphic Geology, 2008, 26, 717-739.	3.4	102
23	Metamorphism, melting, and channel flow in the Greater Himalayan Sequence and Makalu leucogranite: Constraints from thermobarometry, metamorphic modeling, and U-Pb geochronology. Tectonics, 2010, 29, n/a-n/a.	2.8	102
24	Dehydration melting and the granulite transition in metapelites from southern Namaqualand, S. Africa. Contributions To Mineralogy and Petrology, 1984, 88, 269-275.	3.1	98
25	Metastability of granulites and processes of eclogitisation in the UHP region of western Norway. Journal of Metamorphic Geology, 2001, 19, 609-625.	3.4	88
26	Attenuation and excision of a crustal section during extensional exhumation: the Carratraca Massif, Betic Cordillera, southern Spain. Journal of the Geological Society, 1999, 156, 149-162.	2.1	86
27	The high-pressure to ultrahigh-pressure eclogite transition in the Western Gneiss Region, Norway. European Journal of Mineralogy, 2000, 12, 667-687.	1.3	86
28	Structure of the Main Central Thrust zone and extrusion of the High Himalayan deep crustal wedge, Kishtwar–Zanskar Himalaya. Journal of the Geological Society, 2001, 158, 637-652.	2.1	85
29	Metamorphic history of the South Tibetan Detachment System, Mt. Everest region, revealed by RSCM thermometry and phase equilibria modelling. Journal of Metamorphic Geology, 2011, 29, 561-582.	3.4	84
30	Anatomy, age and evolution of a collisional mountain belt: the Baltoro granite batholith and Karakoram Metamorphic Complex, Pakistani Karakoram. Journal of the Geological Society, 2010, 167, 183-202.	2.1	81
31	Quantifying Barrovian metamorphism in the Danba Structural Culmination of eastern Tibet. Journal of Metamorphic Geology, 2013, 31, 909-935.	3.4	81
32	Metamorphic History of Sapphirine-bearing and Related Magnesian Gneisses from Namaqualand, South Africa. Journal of Petrology, 1986, 27, 541-565.	2.8	79
33	A geochronological and petrological study of anatectic paragneiss and associated granite dykes from the <scp>D</scp> ay <scp>N</scp> ui <scp>C</scp> on <scp>V</scp> oi metamorphic core complex, <scp>N</scp> orth <scp>V</scp> ietnam: constraints on the timing of metamorphism within the <scp>R</scp> ed <scp>R</scp> ietnam: constraints on the timing of metamorphism within the <scp>R</scp> ed <scp>R</scp> ietnam: constraints on the timing of metamorphism within the <scp>R</scp> ed <scp>R</scp> ietnam: constraints on the timing of metamorphism within the <scp>R</scp> ed <scp>R</scp> ietnam: constraints on the timing of metamorphism within the <scp>R</scp> ed <scp>R</scp> ietnam: constraints on the timing of metamorphism within the <scp>R</scp> ed <scp>R</scp> ietnam: constraints on the timing of metamorphism within the <scp>R</scp> ed <scp>R</scp> ietnam: constraints on the timing of metamorphism within the <scp>R</scp> ed <scp>R</scp> ietnam: constraints on the timing of metamorphism within the <scp>R</scp> ed <scp>R</scp> ietnam: constraints on the timing of metamorphism within the <scp>R</scp> ed <scp>R</scp> ietnam: constraints on the timing of metamorphism within the <scp>R</scp> ed <scp>R</scp> ietnam: constraints on the timing of metamorphism within the <scp>R</scp> ed <scp>R</scp> ietnam: constraints on the timing of metamorphism within the <scp>R</scp> ed <scp>ed <scp>R</scp>ed <scp>R</scp></scp>	3.4	79
34	Structure of the metamorphic sole to the Oman Ophiolite, Sumeini Window and Wadi Tayyin: implications for ophiolite obduction processes. Geological Society Special Publication, 2014, 392, 155-175.	1.3	76
35	Dating the subduction of the Arabian continental margin beneath the Semail ophiolite, Oman. Geology, 2003, 31, 889.	4.4	74
36	Phase relations of osumilite and dehydration melting in pelitic rocks: a simple thermodynamic model for the KFMASH system. Contributions To Mineralogy and Petrology, 1996, 124, 383-394.	3.1	69

#	Article	IF	CITATIONS
37	A comparison of observed and thermodynamically predicted phase equilibria and mineral compositions in mafic granulites. Journal of Metamorphic Geology, 2019, 37, 153-179.	3.4	66
38	Probing the basement of southern Tibet: evidence from crustal xenoliths entrained in a Miocene ultrapotassic dyke. Journal of the Geological Society, 2009, 166, 45-52.	2.1	61
39	Phase equilibria modelling of retrograde amphibole and clinozoisite in mafic eclogite from the Tso Morari massif, northwest India: constraining the <i>P</i> – <i>T</i> – <i>M</i> (H ₂ O) conditions of exhumation. Journal of Metamorphic Geology, 2014, 32, 675-693.	3.4	59
40	Pleistocene melting and rapid exhumation of the Nanga Parbat massif, Pakistan: Age and P–T conditions of accessory mineral growth in migmatite and leucogranite. Earth and Planetary Science Letters, 2009, 288, 408-420.	4.4	57
41	Monazite geochronology and petrology of kyanite- and sillimanite-grade migmatites from the northwestern flank of the eastern Himalayan syntaxis. Gondwana Research, 2014, 26, 323-347.	6.0	55
42	Chapter 12 Tectonic and metamorphic evolution of the Mogok Metamorphic and Jade Mines belts and ophiolitic terranes of Burma (Myanmar). Geological Society Memoir, 2017, 48, 261-293.	1.7	50
43	Metamorphic evidence for the heating and cooling path of Namaqualand granulites. Geological Society Special Publication, 1989, 43, 357-363.	1.3	48
44	Evolution and chronology of the Pangong Metamorphic Complex adjacent to the Karakoram Fault, Ladakh: constraints from thermobarometry, metamorphic modelling and U–Pb geochronology. Journal of the Geological Society, 2009, 166, 919-932.	2.1	48
45	Combined thermobarometry and geochronology of peraluminous metapelites from the Karakoram metamorphic complex, North Pakistan; New insight into the tectonothermal evolution of the Baltoro and Hunza Valley regions. Journal of Metamorphic Geology, 2012, 30, 793-820.	3.4	48
46	An integrated tectonothermal model for the evolution of the High Himalaya in western Zanskar with constraints from thermobarometry and metamorphic modeling. Tectonics, 2001, 20, 810-833.	2.8	43
47	Structure and metamorphism beneath the obducting Oman ophiolite: Evidence from the Bani Hamid granulites, northern Oman mountains. , 2015, 11, 1812-1836.		43
48	Muscovite dehydration melting: Reaction mechanisms, microstructures, and implications for anatexis. Journal of Metamorphic Geology, 2020, 38, 29-52.	3.4	43
49	U–Pb zircon geochronology and phase equilibria modelling of a mafic eclogite from the Sumdo complex of south-east Tibet: Insights into prograde zircon growth and the assembly of the Tibetan plateau. Lithos, 2016, 262, 729-741.	1.4	41
50	Thermal and mechanical models for the structural and metamorphic evolution of the Zanskar High Himalaya. Geological Society Special Publication, 1999, 164, 139-156.	1.3	38
51	Metamorphic constraints on the tectonic evolution of the High Himalaya in Nepal: the art of the possible. Geological Society Special Publication, 2019, 483, 325-375.	1.3	38
52	Partially Melted Crustal Xenoliths as a Window into Sub-Volcanic Processes: Evidence from the Neogene Magmatic Province of the Betic Cordillera, SE Spain. Journal of Petrology, 2010, 51, 973-991.	2.8	37
53	Exhumation-Driven Devolatilization as a Fluid Source for Orogenic Gold Mineralization at the Damang Deposit, Ghana. Economic Geology, 2015, 110, 1009-1025.	3.8	37
54	Two-stage cooling history of pelitic and semi-pelitic mylonite (sensu lato) from the Dongjiu–Milin shear zone, northwest flank of the eastern Himalayan syntaxis. Gondwana Research, 2015, 28, 509-530.	6.0	36

#	Article	IF	CITATIONS
55	Oxidized eclogites and garnet-blueschists from Oman: P?T path modelling in the NCFMASHO system. Journal of Metamorphic Geology, 2006, 24, 061107121521004-???.	3.4	35
56	The History of Granulite-Facies Metamorphism and Crustal Growth from Single Zircon U-Pb Geochronology: Namaqualand, South Africa. Journal of Petrology, 1999, 40, 1747-1770.	2.8	31
57	Constraints on the timing of late-Eburnean metamorphism, gold mineralisation and regional exhumation at Damang mine, Ghana. Precambrian Research, 2014, 243, 18-38.	2.7	29
58	Quantifying the <i>P–T–t</i> conditions of north–south Lhasa terrane accretion: new insight into the preâ€Himalayan architecture of the Tibetan plateau. Journal of Metamorphic Geology, 2015, 33, 91-113.	3.4	28
59	Kornerupine in Mg-Al-rich gneisses from Namaqualand, South Africa: mineralogy and evidence for late-metamorphic fluid activity. Contributions To Mineralogy and Petrology, 1985, 91, 369-382.	3.1	27
60	Geochemistry and origin of cordierite-orthoamphibole/orthopyroxene-phlogopite rocks from Namaqualand, South Africa. Chemical Geology, 1990, 85, 77-100.	3.3	26
61	Controls on the rheological properties of peridotite at a palaeosubduction interface: A transect across the base of the Oman–UAE ophiolite. Earth and Planetary Science Letters, 2018, 491, 193-206.	4.4	26
62	Thermal History and Tectonic Setting of the Namaqualand Granulites, Southern Africa: Clues to Proterozoic Crustal Development. , 1990, , 243-256.		23
63	Subduction zone polarity in the Oman Mountains: implications for ophiolite emplacement. Geological Society Special Publication, 2003, 218, 467-480.	1.3	23
64	Compressional origin of the Naxos metamorphic core complex, Greece: Structure, petrography, and thermobarometry. Bulletin of the Geological Society of America, 2020, 132, 149-197.	3.3	21
65	Miocene magmatism in the Western Nyainqentanglha mountains of southern Tibet: An exhumed bright spot?. Lithos, 2016, 245, 147-160.	1.4	20
66	The Age, Origin, and Emplacement of the Tsiknias Ophiolite, Tinos, Greece. Tectonics, 2020, 39, e2019TC005677.	2.8	16
67	Reply to Comment by F. Boudier and A. Nicolas on "Dating the geologic history of Oman's Semail Ophiolite: insights from U–Pb geochronology―by C.J. Warren, R.R. Parrish, M.P. Searle and D.J. Waters. Contributions To Mineralogy and Petrology, 2007, 154, 115-118.	3.1	15
68	The application of P–T–X(<scp>CO</scp> ₂) modelling in constraining metamorphism and hydrothermal alteration at the <scp>D</scp> amang gold deposit, <scp>G</scp> hana. Journal of Metamorphic Geology, 2013, 31, 937-961.	3.4	14
69	Prismatine and ferrohögbomite-2N2S in granulite-facies Fe-oxide lenses in the Eastern Ghats Belt at Venugopalapuram, Vizianagaram district, Andhra Pradesh, India: do such lenses have a tourmaline-enriched lateritic precursor?. Mineralogical Magazine, 2003, 67, 1081-1098.	1.4	12
70	Structural and thermal evolution of the South Tibetan Detachment shear zone in the Mt Everest region, from the 1933 sample collection of L. R. Wager. Geological Society Special Publication, 2019, 478, 335-372.	1.3	12
71	Two episodes of monazite crystallization during metamorphism and crustal melting in the Everest region of the Nepalese Himalaya. Geology, 2000, 28, 403-406.	4.4	12
72	Crustal melt granites and migmatites along the Himalaya: melt source, segregation, transport and granite emplacement mechanisms. , 2010, , .		11

#	Article	IF	CITATIONS
73	Reply to: Comment by Gray, Gregory and Miller on "Structural evolution, metamorphism and restoration of the Arabian continental margin, Saih Hatat region, Oman Mountains― Journal of Structural Geology, 2005, 27, 375-377.	2.3	10
74	The Cycladic Blueschist Unit on Tinos, Greece: Cold NE Subduction and SW Directed Extrusion of the Cycladic Continental Margin Under the Tsiknias Ophiolite. Tectonics, 2020, 39, e2019TC005890.	2.8	10
75	Protolith lithostratigraphy of the Greater Himalayan Series in Langtang, Nepal: implications for the architecture of the northern Indian margin. Geological Society Special Publication, 2019, 483, 281-304.	1.3	9
76	Burial, Accretion, and Exhumation of the Metamorphic Sole of the Omanâ€UAE Ophiolite. Tectonics, 2021, 40, e2020TC006392.	2.8	9
77	EBSDâ€based criteria for coesiteâ€quartz transformation. Journal of Metamorphic Geology, 2021, 39, 165-180.	3.4	6
78	Phase equilibria and microstructural constraints on the highâ€ <i>T</i> building of the Kohistan island arc: The Jijal garnet granulites, northern Pakistan. Journal of Metamorphic Geology, 2022, 40, 145-174.	3.4	6
79	Telescoping of isotherms beneath the South Tibetan Detachment, Mount Everest Massif: implications for magnitude of internal flow during extrusi on of the Greater Himalayan Slab. Himalayan Journal of Sciences, 2008, 5, 86-87	0.3	5